ORIGINAL ARTICLE

Removal of manganese(II) ions from aqueous solutions by adsorption on activated carbon derived a new precursor: *Ziziphus spina-christi* seeds

Abdessalem Omri *, **Mourad Benzina**

Laboratory of Water-Energy-Environment (LR3E), Code: AD-10-02, National School of Engineers of Sfax, University of Sfax, BP W, 3038 Sfax, Tunisia

Abstract   In this paper, activated carbon was prepared from *Ziziphus* spina-christi seeds (ZSAC) to remove Mn(II) from aqueous solutions. To characterize the adsorptive characteristics of the produced active carbon, surface area was calculated using the standard Brunauer–Emmet–Teller method. The microstructures of the resultant activated carbon were observed by with scanning electron micrographs. Chemical characterization of the surface resultant activated carbon was studied by Fourier Transform Infrared Spectroscopy. The effects of pH, initial metal ion concentration and temperature on the adsorption performance of ZSAC for Mn(II) ions were examined by batch method. The adsorption equilibrium data were analyzed by Langmuir, Freundlich and Temkin isotherm models. We concluded that maximum adsorption capacity of manganese calculated from Langmuir isotherm was around 172 mg/g.

1. Introduction

Manganese is the second most abundant metal in nature. Its most common mineral is pyrolusite (MnO_2). It is an essential metal for the human system and enzymes activation. It has a variety of applications in ceramics, dry battery cells and electrical coils; it is also an alloying element. In addition to the disposal of untreated discharge from above the applications into water, another major source of pollution of the manganese is burning of coal and oil [1]. Because of the toxicity and non-degradable nature of metallic species, scientists the world over have carried out significant work on their removal from aqueous solutions and industrial effluents. Membrane filtration [2,3], chemical precipitation [3], ion exchange [4], silica [5], adsorption on activated carbon [6], etc., are among the commonly used methodologies for this purpose. The use of activated carbons to remove Mn(II) from water was proposed because of their high surface areas and active functional groups [7] leading to a search for low-cost adsorbents in recent years. Indeed activated carbon production from agricultural waste for example, has two advantages. First, waste material

---

* Corresponding author. Tel.: +216 96803179.
E-mail address: omriabdesslem@yahoo.fr (A. Omri).
Peer review under responsibility of Faculty of Engineering, Alexandria University

is converted to useful, value-added adsorbents. Disposal of agricultural by-products has become a major costly waste disposal problem. Second, produced activated carbons are used for removing organic chemicals and metals from wastewater [8]. Corn cob [9,10], flamboyant pods [11], apricot stone [12,13], almond shell, nut shell, peach stone [13,14], oat hulls, coconut husk [15], coconut shell [16,17], hazelnut shell [14], grape seed [18], olive stone [19] and *Rosa canina* sp. seeds [20] have been used for activated carbon production. *Ziziphus* spina-christi is a plant that grows into a tree with thorny branches and is used as a hedge to form defensive fences for cattle. The fruit has a sweet edible pulp, the leaves are applied locally to sores, and the roots are used to cure and prevent skin diseases [21–23]. The literature does not show research about preparation of activated carbon from *Z.* spina-christi seeds.

In the present study, ZSAC prepared by chemical activation with KOH was characterized and used as an adsorbent to remove Mn(II) from aqueous solutions. The adsorption of manganese ions onto activated carbons was studied in batch equilibrium conditions. The effects of different parameters including pH, initial metal ion concentration and temperature were investigated. Langmuir, Freundlich and Temkin isotherms were used to analyze the equilibrium data.

2. Experimental procedure

2.1. Materials

Z. spina-christi seeds used in this study were collected from Sidi Bouzid, Tunisia. All the reagents used were of analytical grade. The impregnating agent for the chemical activation of the seeds was potassium hydroxide. The aqueous solution of Mn(II) was prepared by dissolving manganese sulfate in double distilled water. The pH of the solution was adjusted using 0.01 N HCl or 0.01 N NaOH.

2.2. Activated carbon preparation

Z. spina-christi seeds were dried at 110 °C for 24 h, ground and granulometrically separated. The material, which had particle size between 1 and 2 mm, was placed in a vertical stainless steel reactor and heated in a furnace at a rate of 10 °C/min from room temperature to 600 °C and maintained at this temperature for 1.5 h. The obtained char was mixed with water and KOH with the weight ratio of water/KOH/char equal to 3/4/1, with constant mechanical stirring for 6 h and a temperature of 85 °C. The impregnated char was dried overnight at 120 °C. The reactor containing the dry mixture was set into a furnace under N_2 flow of 100 cm^3/min, and heated at a rate of 10 °C/min to the final temperature of 700 °C, which was maintained for 2 h. All the activated samples were washed with water, poured into 0.1 mol/L HCl and stirred for 1 h to eliminate the residual alkali [24]. Then, the samples were washed with hot distilled water until the pH of the filtrating solution was neutral [25]. The produced activated carbon was then dried at 105 °C overnight, ground and sifted to obtain a powder with a particle size smaller than 45 μm; it was finally kept in a hermetic bottle for subsequent uses.

2.3. Textural and chemical characterization

2.3.1. Specific surface area

The specific surface (S_{BET}) of activated carbon is determined by a Micrometrics apparatus (ASAP 2010) by adsorption of nitrogen at 77 K according to the traditional method of Brunauer Emmet and Teller or BET [26].

2.3.2. Iodine number

The iodine number (mg/g of activated carbon) was evaluated using the procedure proposed by the Standard Test Method (ASTM D 4607-86). The activated carbon (approximately 0.3–0.6 g) was placed in a 250 mL dry Erlenmeyer flask, and was fully wetted with 10 mL HCl 5%. Then 100 mL of iodine solution (0.1 M) were poured into the flask, and the mixture was vigorously shaken for 30 s. After a quick filtration, 50 mL of the solutions were titrated with sodium thiosulfate (0.1 M) until the solution became pale yellow. Two milliliters of starch indicator solution (1 g/L) were added, and the titration was continued with sodium thiosulfate until the solution became colorless. The concentration of iodine in the solution was thus calculated from the total volume of sodium thiosulfate used.

2.3.3. IR spectroscopy analysis

The surface functional groups and structure were studied by FTIR spectroscopy. The FTIR spectra of the raw material and the resulting activated carbon were recorded between 500 and 4000 cm^{-1} in a NICOET spectrometer.

2.3.4. Thermogravimetric analysis

Thermogravimetric analysis of the activated carbon was performed in a Perkin–Elmer TG/DTA apparatus at a nitrogen flow rate of 100 mL/min and a heating rate of 10 °C/min up to 600 °C.

2.3.5. Morphology analysis

In order to know the structure sight of the activated carbon, Scanning Electron Microscopy (SEM) was employed to visualize sample morphology. In the present work, the activated carbon prepared was analyzed by this technique using a Philips XL30 equipped with an analyzer EDAX (Energy Dispersive Analysis of Analysis of X Rays) to study the surface morphology of the ZSAC and qualitative elemental analysis.

2.4. Batch adsorption experiments

The effects of experimental parameters such as initial metal ion concentration (20–140 mg/L), pH (2.5–6.5) and temperature (25–40 °C) on the adsorptive removal of Mn(II) ions were studied in a batch mode of operation for a specific period of contact time for 180 min. All adsorption experiments were conducted in 250 mL conical flasks, adding 100 mL of manganese solution (with desired concentration and pH) and 75 mg of ZSAC, and then mechanically agitating them in an isothermal water bath shaker at 200 rpm for the wished temperature. After filtration through the filter paper, Mn(II) ions remaining in the solution were determined by ZEENIT Atomic Absorption. The amount of adsorbed manganese per gram ZSAC at

equilibrium, q_e (mg/g), and the removal percentage, (% removal), were calculated using the following equations:

$$q_e = \frac{(C_0 - C_e) \cdot V}{m} \tag{1}$$

$$\% \text{ removal} = \frac{C_0 - C_e}{C_0} \times 100 \tag{2}$$

where C_0 and C_e are the initial and equilibrium concentrations of Mn(II), respectively (mg/L). V is the volume of Mn(II) solution (L) and W is the weight of adsorbent used (g).

3. Results and discussion

3.1. Characteristics of the activated carbon

3.1.1. Physico-chemical properties of the activated carbon

Some properties of the ZSAC are presented in Table 1. The activated carbon product has a surface area about 914.23 m²/g and a porous volume equal to 0.731 cm³/g. The ZSAC is composed mainly of carbon, but also lots of oxygen from many oxygenated surface functions. We also note the presence (15% compared to the carbon content) of potassium due to treatment with potassium hydroxide during the activation step.

3.1.2. FTIR spectroscopic analysis

In this work, infrared spectroscopy was used to obtain information about the chemical structure and functional groups of the raw material and the prepared activated carbon [27,28]. The FTIR spectrum of the *Z. spina-christi* seeds is shown in Fig. 1a. This spectrum is quite similar to that of other lignocellulosic materials such as pistachio-nut shell and rockrose [27,29]. The band located at 3447 cm⁻¹ corresponds to the intra-molecular H-bonded (–OH) [30]. The band observed around 2928 cm⁻¹ is attributed to C–H stretching vibration of –CH₂. The band at 1734 cm⁻¹ is ascribed to carbonyl C=O groups. The skeletal C=C vibrations in aromatic rings cause two bands at 1507 and 1457 cm⁻¹ [31]. The band at 1251 cm⁻¹ may be attributed to esters (e.g. R–CO–O–R′), ethers (e.g. R–O–R′) or phenol groups. The relatively intense band at 1036 cm⁻¹ can be assigned to alcohol groups (R–OH) [32]. The C–H out-of-plane bending in benzene derivative vibrations causes the band at 898 cm⁻¹ [33]. The FT-IR spectra of the activated carbon prepared at 700 °C was shown in Fig. 1b. The bands at 3429 and 1080 cm⁻¹ were assigned to O–H bonds and C–OH stretching of phenolic groups, respectively [34]. According to Montes-Moran et al. [35], the bands observed in the region between 1700 cm⁻¹ and 1490 cm⁻¹ were attributed to C=C symmetrical stretching of pyrone groups
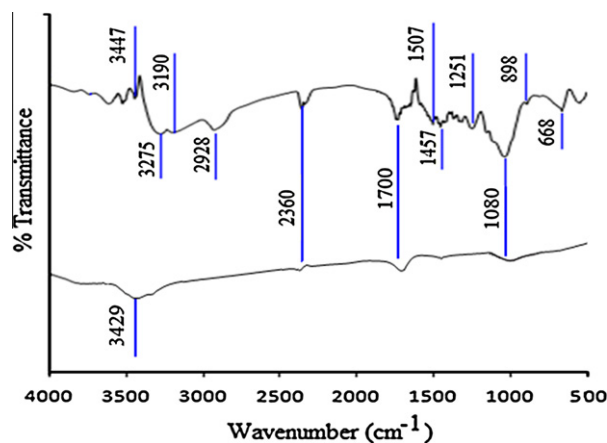

Figure 1 FTIR spectra of (a) *Ziziphus spina-christi* seeds and (b) ZSAC.

and C=O of carboxylic groups. Moreover, Chiang et al. [36] noted that the alkaline treatment increased the amount of oxygen functional groups, especially, phenolic groups. In addition, carbon skeleton vibrations, which are characteristic in activated carbon, were observed.

3.1.3. Thermogravimetric analysis

The TG-DTG graphs for the prepared activated carbon and the raw material are shown in Figs. 10 and 11. The TG curves given in Fig. 2 show that at low temperatures (up to 120 °C), the raw material presents a slight mass loss (7%) due to the elimination of moisture. Then, up to approximately 230 °C, the sample mass remains nearly constant, decreasing markedly between 250 and 410 °C due to the release of the volatile matter occurs from degradation of cellulose and hemicelluloses from the precursor (65% mass loss) [37,38]. At 450 °C, the remaining material corresponds to 21% of the initial material. At higher temperatures, the sample mass decreases slightly up to 600 °C, remaining only 18% of the initial mass indicating the decomposition of lignin, which was a structure with higher stability [39]. Moreover, the ZSAC thermogram showed a final average yield of 81% for heating up to 600 °C, indicating a high thermal resistance. Fig. 3 shows the DTG thermogram
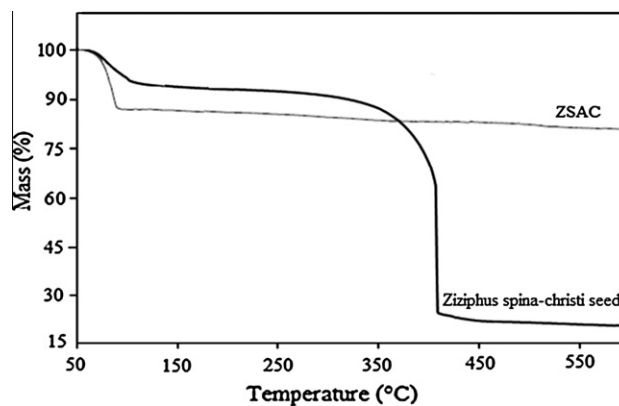
Table 1 Some properties of the ZSAC.

Parameter	Value
Specific surface area (m²/g)	914.23
Porous volume (cm³/g)	0.731
Carbon (%)	64.152
Oxygen (%)	8.994
Potassium (%)	9.731
Iodine number (mg/g)	797

Figure 2 TG thermogram of *Ziziphus spina-christi* seeds and ZSAC.
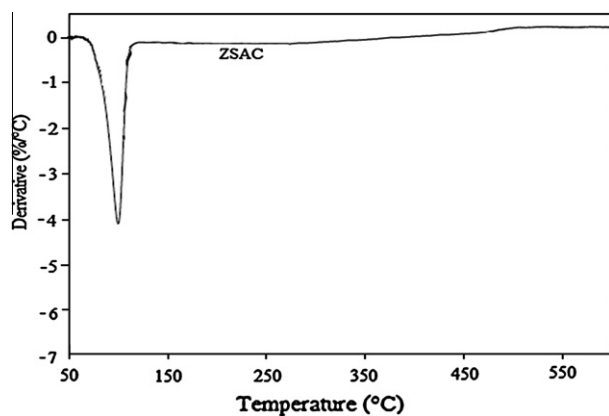
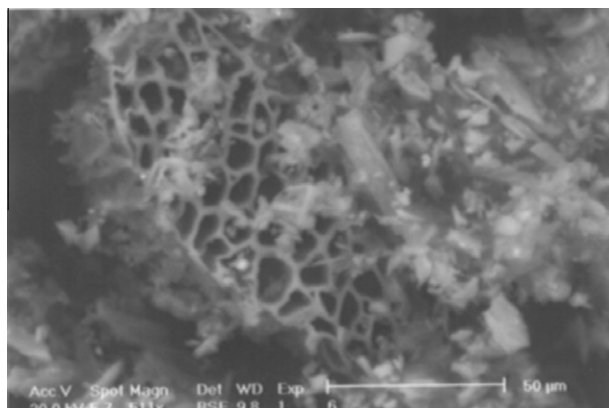**Figure 3** DTG thermogram of ZSAC.
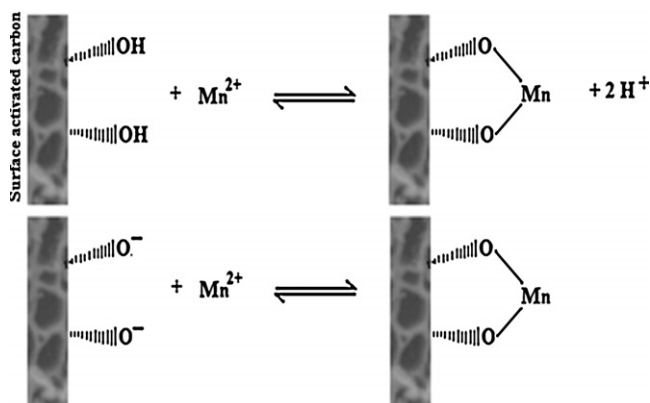

Figure 4 SEM image of ZSAC.

Figure 5 Possible mechanisms of ion exchange.

of ZSAC, the peak observed between 60 and 120 °C is due to moisture elimination.

3.1.4. Surface morphology

SEM image of the ZSAC is shown in Fig. 4. The external surfaces of these ZSAC show large cavities and are very irregular, indicating that the porosity of the material was produced by an aggressive attack of the reagent (KOH) during activation.
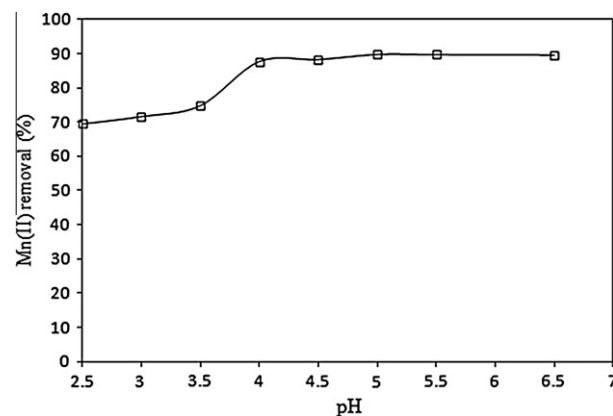

Figure 6 Effect of pH on removal of Mn(II) (initial concentration 50 mg/L; temperature 25 °C).

Activation at 700 °C with KOH resulted in the creation of more pores and a substantial removal of volatiles [40]. Large and well-developed pores were clearly found on the surface of the activated carbon. Pore development in the ZSAC during pyrolysis was also important as this would enhance the surface area and pore volume of the activated carbon by promoting the diffusion of KOH molecule into the pores and thereby increasing the KOH–carbon reaction, which would then create more pores in the activated carbon.

Activation with KOH represents the intercalation of potassium between the layers of graphenes and the hydrogen formation, which causes to minimize the quantity of surface oxygen catalytically active [41].

3.2. Mechanism of adsorption

The surface of the prepared activated carbon contains functional groups of oxygen and aromatic compounds. These groups can be involved in chemical bonding and are responsible for the cation exchange capacity of the ZSAC. Thus, the ZSAC/manganese reaction may be represented in two ways (Fig. 5). According to this figure, possible mechanisms of ion exchange can be considered a manganese ion (Mn^{2+}) which attaches itself to two adjacent hydroxyl groups and two-oxyl groups which could donate two pairs of electrons to metal ions, forming four coordination number compounds and releasing two hydrogen ions into solution.

3.3. Effect of pH on removal of Mn(II)

It is well known that the adsorption of heavy metal ions depends on the pH of the aqueous solution. Fig. 6 indicates the effect of pH on the removal of manganese(II) ions onto ZSAC from aqueous solutions. The solution pH was varied from 2.5 to 6.5. While Mn(II) removal was 69.52% at pH 2.5, it was 87.69% for adsorbent at pH 4. For pH > 4, the maximum uptake is attained and is maintained constant. Maximum adsorption at acidic pH indicates that low pH leads to an increase in H^+ ions on the carbon surface, resulting in significantly strong electrostatic attraction between positively charged ZSAC surface and manganese ions. This might be attributed to the partial hydrolysis of Mn(II) ions with
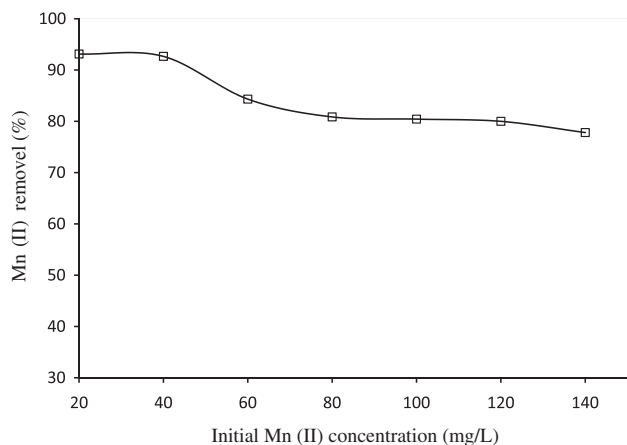
Figure 7 Effect of initial concentration on removal of Mn(II) (pH = 4; temperature 25 °C).
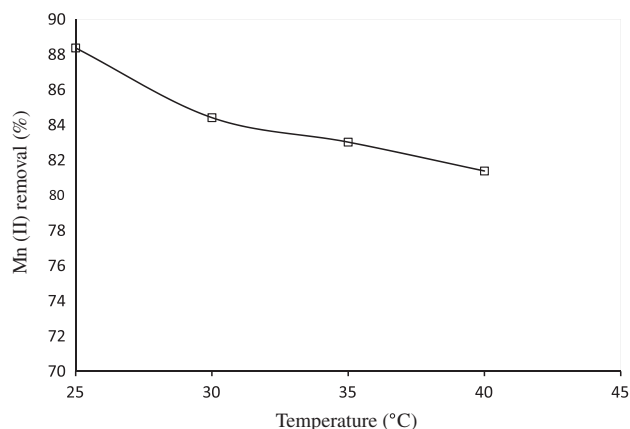

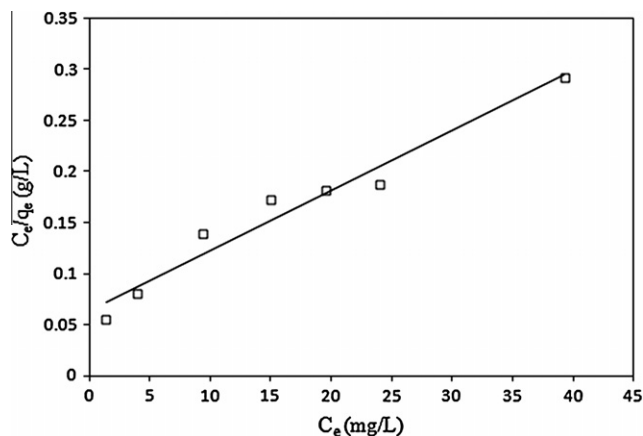**Figure 8** Effect of temperature on removal of Mn(II) (initial concentration 50 mg/L; pH = 4).

Figure 9 Langmuir isotherm for Mn(II) adsorption onto ZSAC at 25 °C.

increasing pH, bringing about the formation of complexes with OH$^-$ such as Mn(OH)$^+$, Mn(OH)$_2$, Mn$_2$(OH)$_3^+$, Mn$_2$OH^{3+},

and Mn(OH)$_4^{2-}$ species in solution [42]. As a result, Mn-hydroxyl species may participate in the adsorption and/or precipitation onto the adsorbent structure. The maximum removal percentage occurs at pH = 4 and hence it was taken as the optimal value for further adsorption studies.

3.4. Effect of initial Mn(II) concentration on the removal of manganese

The effect of the initial concentration on Mn(II) was investigated in the range 20–140 mg/L with a pH value fixed at 4. The results are shown in Fig. 7. If the mass of ZSAC in the suspension is equal to 75 mg, 93.12% of the initial Mn(II) with a concentration of 20 mg/L is removed. For example, while the amount adsorbed was 24.83 mg/g at the initial Mn(II) concentration of 20 mg/L, it increased to 145.24 mg/g at the initial Mn(II) concentration of 140 mg/L. At lower metal concentration, the ratio of the number of moles of manganese in a solution to the available surface area is low and hence adsorption is independent of the initial concentration. At higher concentration, the number of available sites for adsorption decreases and, hence, metal removal is dependent on the initial concentration.

3.5. Effect of temperature on removal of Mn(II)

Temperature has a pronounced effect on the removal of pollutant species from aqueous solutions with most adsorption processes being exothermic in nature [43]. Investigation for the present process also revealed its exothermic nature [44]. The removal of Mn(II) decreased from 88.37% to 81.38% by increasing the temperature from 25 to 40 °C (Fig. 8). The variation in the removal may be a result of the enhanced escaping tendency of pollutant species at increasing temperatures. The possibility of increased solubility at higher temperatures and hence a lower adsorption can also not be ruled out.

3.6. Adsorption isotherms

Adsorption equilibrium data were fitted to the Langmuir, Freundlich and Temkin isotherms at a temperature of 25 °C and with pH = 4. Langmuir isotherm is based on the monolayer adsorption of manganese ions on the surface of carbon sites and is expressed in the linear form as [45]

$$\frac{C_e}{q_e} = \frac{1}{Q_0 b} + \frac{C_e}{Q_0} \tag{3}$$

where C_e is the equilibrium concentration (mg/L) and q_e the amount adsorbed at equilibrium (mg/g). The Langmuir constants Q_0 (mg/g) represent the monolayer adsorption capacity and b (L/mg) relates to the heat of adsorption. A plot of C_e/q_e versus C_e gives a straight line of slope $1/Q_0$ and intercepts $1/Q_0 b$.

Freundlich isotherm describes the heterogeneous surface energies by multilayer adsorption and is expressed in linear form as [46]

$$\log q_e = \log K_F + \left(\frac{1}{n}\right) \log C_e \tag{4}$$

The constants K_F (mg/g (L/mg)$^{1/n}$) and $1/n$ of the Freundlich model are those indicative of the relative adsorption capacity
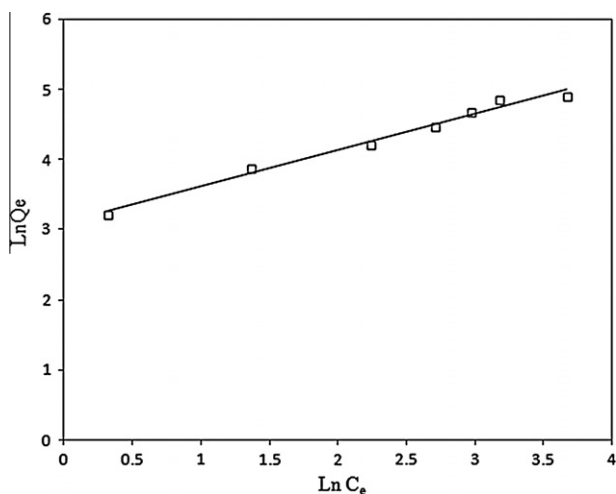
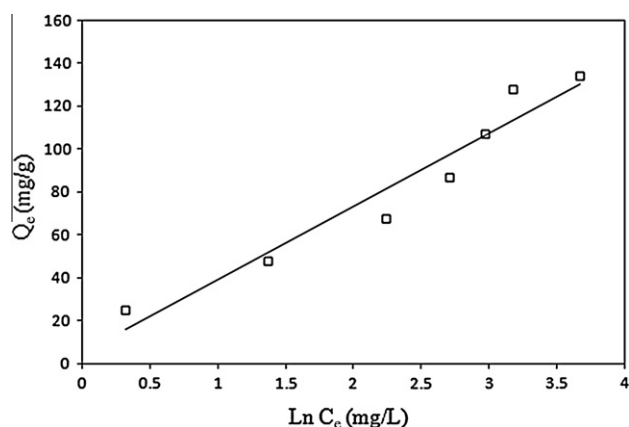**Figure 10** Freundlich isotherm for Mn(II) adsorption onto ZSAC at 25 °C.

Figure 11 Temkin isotherm for Mn(II) adsorption onto ZSAC at 25 °C.

Table 2 Langmuir, Freundlich and Temkin isotherm parameters and correlation coefficients for the adsorption of Mn(II) in aqueous solutions onto ZSAC at 25 °C.

Isotherms	Mn(II) constants
Langmuir isotherm	
Q_0 (mg/g)	172.413
b (L/mg)	0.09
R^2	0.959
Freundlich isotherm	
K_F (mg/g) (L/mg)$^{1/n}$	21.968
$1/n$	0.519
R^2	0.984
Temkin isotherm	
b_T (J/mol)	72.378
A (L/g)	1.148
R^2	0.937

Table 3 Comparison of adsorption capacity with other adsorbents.

Adsorbent	Adsorbent dosage (g/L)	Q_0 (mg/g)	Reference
Activated carbon immobilized by tannic acid	2	1.73	[50]
Pecan nutshell biosorbent	5	103.8	[31]
Pithacelobium dulce carbon	0.1	0.415	[51]
Crab shell particles	5	69.9	[52]
Thermally decomposed leaf	10	66.57	[53]
Natural zeolitic tuff	10	10	[54]
Activated carbon of *Ziziphus spina-christi* seeds	0.75	172.413	This study

of the adsorbent and the intensity of the adsorption, respectively. For values in the range $0.1 < 1/n < 1$, adsorption is favorable [47]. The greater the values of $1/n$, the better the favorability of adsorption.

Temkin isotherm based on the heat of adsorption of the ions, which is due to the adsorbate and adsorbent interactions taken in linear form, is given by [48]

$$q_e = \left(\frac{RT}{b_T}\right) \ln A + \left(\frac{RT}{b_T}\right) \ln C_e \qquad (5)$$

where $B = RT/b_T$, b_T is the Temkin constant related to the heat of sorption (J/mol), A is the Temkin isotherm constant (L/g), R the gas constant (8.314 J/mol K) and T the absolute temperature (K).

The linear plot of specific adsorption (C_e/q_e) against the equilibrium concentration (C_e) for Langmuir model, ($\log q_e$) against the ($\log C_e$) for Freundlich model and (q_e) against the ($\ln C_e$) for Temkin models are shown in Figs. 9–11. The constants calculated from the linear forms of the three isotherms are given in Table 2.

As can be seen in Table 2, the Freundlich isotherm model had highest values of regression coefficients when compared to the rest of isotherm models, this model was more suitable for the adsorption equilibrium of Mn(II). According to Trybal [49] it has been shown using mathematical calculations that n values between 1 and 10 represent beneficial adsorption.

The adsorption capacity (Q_0) of Mn(II) onto ZSAC was compared with other adsorbents reported in literature and is shown in Table 3. It can be seen from the table that ZSAC shows the very high adsorption capacity with respect to other adsorbents, revealing that ZSAC can be considered a viable adsorbent for the removal of Mn(II) from aqueous solutions.

4. Conclusion

The present study demonstrates that the prepared activated carbon from *Z. spina-christi* seeds is an effective adsorbent for the removal of Mn(II) from aqueous solutions. Scanning Electron Microscopy and Fourier Transform Infrared Spectroscopy investigations were evidenced the presence of a porous structure and different functionalities on the ZSAC surface. Adsorption of Mn(II) was influenced by various parameters such as initial pH, initial concentration of manganese and temperature. The highest removal of Mn(II) was

obtained at pH (pH = 4). The removal efficiency decreased with increased temperature and initial concentrations. The Langmuir, Freundlich and Temkin adsorption isotherm models were used to explain the adsorbate removal. The equilibrium adsorption of Mn(II) over the entire concentration range was best described by the Freundlich isotherm, as indicated by the high values of the correlation coefficients ($R^2 = 0.984$).

Acknowledgements

References

[1] K. Kannan, Fundamentals of Environmental Pollution, S Chand Co. Limited, New Delhi, 1995.
[2] H. Bessbousse, T. Rhlalou, J.F. Verchère, L. Lebrun, Removal of heavy metal ions from aqueous solutions by filtration with a novel complexing membrane containing poly(ethyleneimine) in a poly(vinyl alcohol) matrix, J. Membr. Sci. 307 (2008) 249–259.
[3] M.J. González-Muñoz, M.A. Rodríguez, S. Luque, J.R. Álvarez, Recovery of heavy metals from metal industry wastewaters by chemical precipitation and nanofiltration, Desalination 200 (2006) 742–744.
[4] R. Kiefer, A.I. Kalinitchev, W.H. Höll, Column performance of ion exchange resins with aminophosphonate functional groups for elimination of heavy metals, React. Funct. Polym. 67 (2007) 1421–1432.
[5] C.G. Passos, E.C. Lima, L.T. Arenas, N.M. Simon, B.M. da Cunha, J.L. Brasil, T.M.H. Costa, E.V. Benvenutti, Use of 7-amine-4-azahepthylsilica and 10-amine-4 azadecylsilica xerogels as adsorbent for Pb(II). Kinetic and equilibrium study, Colloids Surf. A 316 (2008) 297–306.
[6] O.S. Amuda, A.A. Giwa, I.A. Bello, Removal of heavy metal from industrial wastewater using modified activated coconut shell carbon, Biochem. Eng. J. 36 (2007) 174–181.
[7] J. Chen, S. Yiacoumi, T.G. Blaydes, Equilibrium and kinetic study of copper adsorption by activated carbon, Sep. Technol. 6 (1996) 133–146.
[8] M.M. Johns, W.E. Marshall, C.A. Toles, Agricultural by-products as granular activated carbons for adsorbing dissolved metals and organics, J. Chem. Technol. Biotechnol. 71 (1998) 131–140.
[9] Y. Sun, P.A. Webley, Preparation of activated carbons from corn cob with large specific surface area by a variety of chemical activators and their application in gas storage, Chem. Eng. J. 162 (2010) 883–892.
[10] W.T. Tsai, C.Y. Chang, S.Y. Wang, C.F. Chang, S.F. Chien, H.F. Sun, Preparation of activated carbons from corn cob catalyzed by potassium salts and subsequent gasification with CO_2, Bioresour. Technol. 78 (2001) 203–208.
[11] A.M.M. Vargas, C.A. Garcia, E.M. Reis, E. Lenzi, W.F. Costa, V.C. Almeida, NaOH-activated carbon from flamboyant (Delonix regia) pods: optimization of preparation conditions using central composite rotatable design, Chem. Eng. J. 162 (2010) 43–50.
[12] K. Gergova, S. Eser, Effects of activation method on the pore structure of activated carbons from apricot stones, Carbon 34 (1996) 879–888.
[13] D. Savova, E. Apak, E. Ekinci, F. Yardım, N. Petrov, T. Budinova, M. Razvigorova, V. Minkova, Biomass conversion to carbon adsorbents and gas, Biomass Bioenergy 21 (2001) 133–142.
[14] W. Heschel, E. Klose, On the suitability of agricultural by-products for the manufacture of granular activated carbon, Fuel 74 (1995) 1786–1791.
[15] I.A.W. Tan, A.L. Ahmad, B.H. Hameed, Optimization of preparation conditions for activated carbons from coconut husk using response surface methodology, Chem. Eng. J. 137 (2008) 462–470.
[16] H.M. Mozammel, O. Masahiro, S.C. Bahattacharya, Activated charcoal from coconut shell using $ZnCl_2$ activation, Biomass Bioenergy 22 (2002) 397–400.
[17] Z. Hu, M.P. Srinivasan, Ni Yaming, Novel activation process for preparing highly microporous and mesoporous activated carbons, Carbon 39 (2001) 877–886.
[18] K. Gergova, N. Petrov, S. Eser, Adsorption properties and microstructure of activated carbons produced from agricultural by-products by steam pyrolysis, Carbon 32 (1994) 693–702.
[19] M.M. Sabio, F.R. Reinoso, Role of chemical activation in the development of carbon porosity, Colloids Surf. 241 (2004) 15–25.
[20] A. Gurses, C. Dogar, S. Karaca, M. Ackyldz, R. Bayrak, Production of granular activated carbon from waste Rosa canina sp. seeds and its adsorption characteristics for dye, J. Hazard. Mater. 131 (2006) 254–259.
[21] C. Sudhersan, J. Hussain, In vitro propagation of a multipurpose tree, Ziziphus spina-christi (L.), Desf, Turk. J. Bot. 27 (2003) 167–171.
[22] E. Lev, Z. Amar, Ethnopharmacological survey of traditional drugs sold in Israel at the end of 20th century, J. Ethnopharmacol. 72 (2000) 191–205.
[23] A.A. Shahat, L. Pieters, S. Apers, N.M. Nazeit, N.S. Abdel-Azim, D.V. Berghe, A.T. Vlietinck, Chemical and biological investigation on Ziziphus spina-christi L, Phytother. Res. 15 (2001) 593–597.
[24] W. Feng-Chin, T. Ru-Ling, J. Ruey-Shin, Preparation of highly microporous carbons from fir wood by KOH activation for adsorption of dyes and phenols from water, Sep. Purif. Technol. 47 (2005) 10–19.
[25] Z. Hu, M.P. Srinivasan, Preparation of high-surface-area activated carbons from coconut shell, Microporous Mesoporous Mater. 27 (1999) 11–18.
[26] S. Braunauer, P. Emmette, E. Teller, Adsorption of gases in multimolecular layers, J. Am. Chem. Soc. 60 (1938) 309–319.
[27] V. Gomez-Serrano, J. Pastor-Villegas, C.J. Duran-Valle, C. Valenzuela-Calahorro, Heat treatment of rockrose char in air. Effect on surface chemistry and porous texture, Carbon 34 (1996) 533–538.
[28] M.S. Solum, R.J. Pugmire, M. Jagtoyen, F. Derbyshire, Evolution of carbon structure in chemically activated wood, Carbon 33 (1995) 1247–1254.
[29] J. Pastor-Villegas, C. Valenzuela-Calahorro, A. Bernalte-Garcia, V. Gomezserrano, Characterisation study of char and activated carbon prepared from raw and extracted rockrose, Carbon 31 (1993) 1061–1069.
[30] H.E.S. Amjad, P.N. Alan, K.A.D. Hafid, P. Suki, C. Neil, Characterization of activated carbon prepared from a single cultivar of Jordanian Olive stones by chemical and physicochemical techniques, J. Anal. Appl. Pyrol. 71 (2004) 151–164.
[31] J.C.P. Vaghetti, E.C. Lima, B. Royer, B.M. da Cunha, N.F. Cardoso, J.L. Brasil, S.L.P. Dias, Pecan nutshell as biosorbent

to remove Cu(II), Mn(II) and Pb(II) from aqueous solutions, J. Hazard. Mater. 162 (2009) 270–280.

[32] R. Baccar, J. Bouzid, M. Feki, A. Montiel, Preparation of activated carbon from Tunisian olive-waste cakes and its application for adsorption of heavy metal ions, J. Hazard. Mater. 162 (2009) 1522–1529.

[33] H. Demiral, I. Demiral, B. Karabacakoglu, F. Tümsek, Production of activated carbon from olive bagasse by physical activation, Chem. Eng. Res. Des. 89 (2011) 206–213.

[34] J.L. Figueiredo, M.F.R. Pereira, M.M.A. Freitas, J.J.M. Órfão, Modification of the surface chemistry of activated carbons, Carbon 37 (1999) 1379.

[35] M.A. Montes-Moran, D. Suarez, J.A. Menendez, E. Fuente, On the nature of basic sites on carbon surfaces: an overview, Carbon 42 (2004) 1219–1225.

[36] H.L. Chiang, C.P. Huang, P.C. Chiang, The surface characteristics of activated carbon as affected by ozone and alkaline treatment, Chemosphere 47 (2002) 257–265.

[37] B. Cagnon, X. Py, A. Guillot, F. Stoeckli, G. Chambat, Contributions of hemicellulose, cellulose and lignin to the mass and the porous properties of chars and steam activated carbons from various lignocellulosic precursors, Bioresour. Technol. 100 (2009) 292–298.

[38] C. Sentorun-Shalaby, M.G. Ucak-Astarlioglu, L. Artok, C. Sarici, Preparation and characterization of activated carbons by one-step steam pyrolysis/activation from apricot stones, Microporous Mesoporous Mater. 88 (2006) 126–134.

[39] B.S. Girgis, A. El-Hendawy, Abdel-Nasser, Porosity development in activated carbons obtained from date pits under chemical activation with phosphoric acid, Mesoporous Mater. 52 (2002) 105–117.

[40] C.L. Aik, Y. Ting, Effect of activation temperature on the textural and chemical properties of potassium hydroxide activated carbon prepared from pistachio-nut shell, J. Colloid Interface Sci. 274 (2004) 594–601.

[41] M.A. Lilllo-Rodenas, J.P. Marco-Lazar, D. Cazorla-Amoros, A. Linares-Solano, Activated carbons prepared by pyrolysis of mixtures of carbon precursor/alkaline hydroxide, J. Anal. Appl. Pyrol. 80 (2007) 166–174.

[42] R.M. Smith, A.E. Martell, Critical Stability Constants, Inorganic Complexes, vol. 4, Plenum Press, New York and London, 1976, pp. 5.

[43] S. Netpradit, P. Thiravetyan, S. Towprayoon, Application of waste metal hydroxide sludge for adsorption of azo reactive dyes, Water Res. 37 (2003) 763–772.

[44] M. Benzina, Contribution to Kinetics and Thermodynamics Study of Organic Vapors Adsorption on Local Clays, Modeling a Fixed Bed Adsorber, Thesis, University of Sciences, Tunis, 1990.

[45] I. Langmuir, The adsorption of gases on plane surfaces of glass, mica and platinum, J. Am. Chem. Soc. 40 (1918) 1361–1403.

[46] H.M.F. Freundlich, Over the adsorption in solution, J. Phys. Chem. 57 (1906) 385–470.

[47] C. Raji, T.S. Anirudhan, Batch Cr(VI) removal by polyacrylamide-grafted sawdust: kinetics and thermodynamics, Water Res. 32 (1998) 3772–3780.

[48] K.K.H. Choy, G. McKay, J.F. Porter, Sorption of acid dyes from effluents using activated carbon, Resour. Conserv. Recycl. 27 (1999) 57–71.

[49] R.E. Trybal, Mass Transfers Operations, third ed., McGraw, New York, 1980.

[50] A. Üçer, A. Uyanik, S.F. Aygün, Adsorption of Cu(II), Cd(II), Zn(II), Mn(II) and Fe(III) ions by tannic acid immobilised activated carbon, Sep. Purif. Technol. 47 (2006) 113–118.

[51] K.A. Emmanuela, A. Veerabhadra Rao, Adsorption of Mn(II) from aqueous solutions using pithacelobium dulce carbon, Rasayan J. Chem. 1 (2008) 840–852.

[52] K. Vijayaraghavan, W. Heng Yun Ni, R. Balasubramanian, Biosorption characteristics of crab shell particles for the removal of manganese(II) and zinc(II) from aqueous solutions, Desalination 266 (2011) 195–200.

[53] L. Zhenze, I. Shigeyoshi, K. Takeshi, I. Toru, T. Xiaowu, T. Qiang, Manganese removal from aqueous solution using a thermally decomposed leaf, J. Hazard. Mater. 177 (2010) 501–507.

[54] N. Rajic, D. Stojakovic, S. Jevtic, N.Z. Logar, J. Kovac, V. Kaucic, Removal of aqueous manganese using the natural zeolitic tuff from the Vranjska Banja deposit in Serbia, J. Hazard. Mater. 172 (2009) 1450–1457.